Available online at www.sciencedirect.com
SCIENCE DIRECT®
Catalysis Today 104 (2005) 131–137
CATALYSIS TODAY
www.elsevier.com/locate/cattod

Oxidative activation of ethane on catalytic modified dense ionic oxygen conducting membranes

M. Rebeilleau-Dassonneville, S. Rosini, A.C. van Veen *, D. Farrusseng, C. Mirodatos

Institut de Recherches sur la Catalyse (CNRS UPR 5401), 2 av. Albert Einstein, F-69626 Villeurbanne Cedex, France

Available online 10 May 2005

Abstract

A reactor using dense mixed ion electron conducting membranes was successfully studied in the oxidative dehydrogenation of ethane to ethylene. Already bare $Ba_{0.5}Sr_{0.5}Co_{0.8}Fe_{0.2}O_{3-\delta}$ membranes allowed reasonable operation with yields beyond state-of-the-art steam cracking. The application of a surface catalyst was found to enhance performance even further. Long term stable operation and ethylene yields of about 75% were observed when using membranes with V/MgO micron grain or Pd nano cluster modified surfaces at temperatures of 1040 or 1050 K, respectively. Being one key factor for the performance of the membrane reactor, the influence of the surface catalysts on the oxygen permeation is reported in a detailed study. Parameters for a model describing the oxygen permeation were determined. The nature of the model indicates the importance of the surface exchange for oxygen permeation, explaining in this way the observed enhancement after application of surface catalysts at the permeate side.

Keywords: Ethane; Ethylene; Oxidative dehydrogenation; Membrane reactor; Surface catalyst

1. Introduction

Ethylene is a key intermediate product in industrial chemistry with worldwide capacities as large as 79.3 Mt/a in 1996 [1] and 70 Mt/a in 2003 [2]. Current ethylene production is based on steam cracking of ethane, naphtha or heavier feed stocks. Main advantages of this short contact time process relate to mature process technology, additional production of hydrogen and layout well adapted to a use of ethane. State of the art is a conversion of 75% at an announced selectivity of 80%, implying a per pass yield of 60% [3,4]. On the other hand, there are major disadvantages since thermodynamics necessitate high temperatures, which involves side reactions like substantial coke formation, hence enforcing frequent discontinuations for reactor clean-up. Moreover, due to the strong endothermic character of the reaction, high heat fluxes need to be transferred from wall burners to the centre of the pyrolysis tubes and energy efficiency becomes a crucial cost factor. A potential alternative to steam cracking is the oxidative dehydrogenation of ethane (ODHE). Indeed, this reaction has the advantage of being exothermic and the presence of oxygen limits coke formation. Unfortunately, formation of hydrogen as coupled product is lost and ethylene yields of current catalysts are too low for commercial applications, as attempts to replace the existing technology would require yields of at least 70%. Furthermore, a use of pure oxygen or enriched air would contribute to increase process costs. However, those former mentioned drawbacks of the oxidative dehydrogenation of ethane might be overcome by membrane reactor technology. The current paper reports on recent advances at laboratory scale indicating significant benefits of the dense mixed ion electron conducting (MIEC) membrane reactor compared to fixed bed reactor operation reported so far in literature [5–11].

The objective of the present work was to explore the potential of surface modified dense membranes, supplying from air ionic oxygen to catalysts placed on the other membrane surface reacting ethane to ethylene. The principle is therefore a combination of catalyst filled or coated membrane reactors recently applied for the production of

* Corresponding author. Tel.: +33 472 44 5482; fax: +33 472 44 5399.
E-mail address: vanveen@catalyse.cnrs.fr (A.C. van Veen).

0920-5861/$ – see front matter © 2005 Elsevier B.V. All rights reserved.
doi:10.1016/j.cattod.2005.03.071

syngas from methane by partial oxidation [12–14] and the (oxidative) dehydrogenation of ethane over unmodified membranes [15,16]. We chose as membrane material a perovskite showing an outstanding performance in terms of oxygen permeation [17,18]. As the studied reaction proceeds at temperatures lower than those for the methane case catalysts were expected to improve the reactor performance. On the other hand, temperatures are higher than those required under conventional ODHE conditions, in order to attain sufficiently high oxygen fluxes through the membrane. This implies that small amounts of catalysts could be sufficient, which might be deposited on the membrane surface to take benefit of the direct supply with more selective ionic oxygen as compared to species derived gas-phase oxygen.

The present report presents the influence of different catalysts on the oxygen permeation in terms of attainable fluxes and performance stability. It also details parameters of a mathematical model describing the oxygen permeation and outlines the effect of catalysts on the membrane surface on the performance in oxygen permeation and dehydrogenation.

2. Experimental

The $Ba_{0.5}Sr_{0.5}Co_{0.8}Fe_{0.2}O_{3-\delta}$ (BSCFO) perovskite powder was prepared by a variant of the so-called citrates method [19]. Briefly, stoichiometric amounts of $Ba(NO_3)_2$, $Sr(NO_3)_2$, $Co(NO_3)_2{\cdot}6H_2O$ and $Fe(NO_3)_3{\cdot}6H_2O$ (purity >99.5%) were fully dissolved in a small amount of distilled water, followed by addition of EDTA and citric acid with the molar ratio perovskite: EDTA: citric acid equal to 1:1.5:3. The obtained purple solution was heated at 373 K and a gel like material was formed by evaporation of water after about 3 h. The gel was then heated at 575 K for 3 h. The obtained foam was calcined at 1173 K for 4 h in air yielding a homogenous perovskite powder. The formation of a pure phase was checked by XRD using a Bruker D5005 system in the 2θ range of 3–80°, a step width of 0.02°, a counting time of 1 s and Cu Kα1+α2 radiation (1.54184 Å). The bulk elementary composition was confirmed by ICP-OES analysis of samples dissolved in a mixture of H_2SO_4 and HNO_3 heated at 523–573 K. The perovskite powder was then ground in mortar, raw membrane discs were pressed at a pressure of 140 MPa and membranes were obtained during densification at 1443 K for 4 h.

Membranes carrying catalysts at the surface of the permeate side were prepared by two techniques. Physical vapor deposition of Pd nano clusters was performed by focusing a Nd-YAG laser onto a single crystal Pd_{100} rod, driven in slow screw motion. Short helium bursts, synchronized with the laser pulses created a cool plasma that expanded at supersonic speed to the exit of the source, forming of a beam of clusters, containing neutral and ionized species. These clusters were injected into a vacuum chamber and deposited on the surface of the dense MIEC disk. The deposition rates were calibrated by a quartz microbalance and adjusted to 5 nm cm^{-2} min^{-1}. These conditions yielded a final membrane surface coverage of about 10% with aggregates having a thickness close to 8 Å. Alternatively, well dispersed micron sized V/MgO grains were coated by a sol–gel based spin casting technique. The needed colloidal suspension with a V:Mg ratio of 1:9 was obtained by mixing respective precursor solutions [20]. A final catalyst loading of about 1 mg/cm^2 was obtained after calcinations and powder reference experiments indicated a high specific catalyst surface area of 75 m^2 g^{-1} even after a treatment at 1073 K. It corresponds to a membrane surface coverage of about 40%.

Oxygen permeation studies and investigations of the ODHE reaction were carried out in a reactor fully described in [19]. Basically, discs (about 1 mm thick) were sealed in between two dense alumina tubes (OD 12 mm, i.d. 8 mm) using gold rings as chemically inert sealant, by heating to 1073 K for one night. The oxygen-rich side was fed at a constant total pressure adjusted to 1.1 bar using typically a constant total flow rate of 50 ml min^{-1} of a mixed O_2 and N_2 stream individually controlled by mass flow controllers. The reaction side was fed either by helium as sweep gas or a mixture of ethane and helium reactant feed. On both membrane sides the gases were preheated while passing the void space between the alumina tube and an inserted quartz tube. To evaluate the performances of different membranes in ODHE respective experiments were performed in the temperature range of 973–1123 K. The reactant side was supplied with a flow of 37 ml min^{-1} C_2H_6/He and the C_2H_6 partial pressure equalled to 0.25 bar. The air side compartment was fed with 50 ml min^{-1} at total pressure of 1.2 bar The reactant gases (O_2, N_2, C_2H_6) and the product gases (H_2, CH_4, CO_2, C_2H_4, C_2H_6 and H_2O) were analyzed by on-line gas chromatography. The carbon balance was kept within 4%. Membrane gas leak free conditions were ensured by monitoring nitrogen concentration on the reacting side.

3. Results and discussion

3.1. Oxygen permeation: experiments and modeling

Oxygen permeation from the air to the reaction side is a key factor in ODHE possibly determining the overall performance of the CMR. Fig. 1 depicts the oxygen permeation for a bare, Pd nano cluster modified and V/MgO micron grain modified membrane as a function of temperature. In addition to measurements using temperature steps, the solid line depicts the performance of a bare membrane when performing continuous measurements during a slow temperature ramp of 0.5 K min^{-1} in the temperature range of 923 K up to 1223 K. In all cases the air side compartment was fed with 50 ml min^{-1}, the permeation side was swept with 30 ml min^{-1} He at a total pressure of

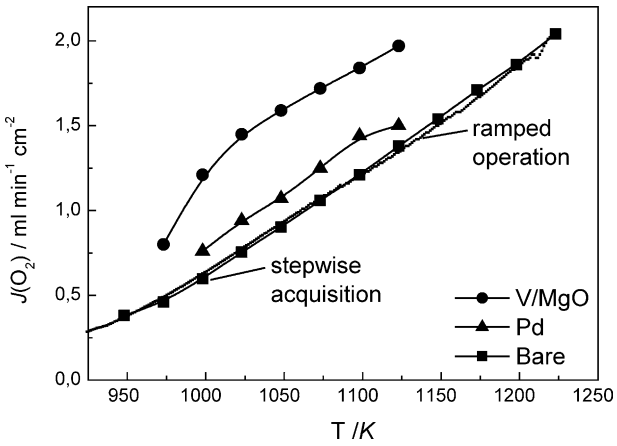

Fig. 1. Oxygen permeation fluxes of a bare (■), Pd nano cluster modified (▲) and V/MgO micron grain modified (●) membrane as a function of temperature. The air side compartment was fed with 50 ml min^{-1}, the permeation side was swept with 30 ml min^{-1} He at total pressure of 1.1 bar on both sides.

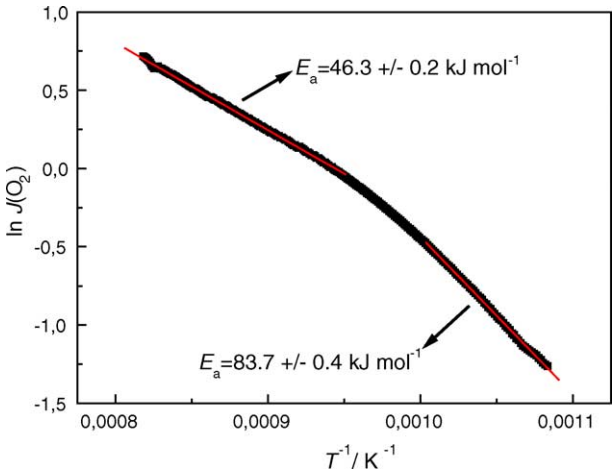

Fig. 2. Determination of the activation energy for oxygen permeation in the case of a bare membrane.

1.1 bar on both sides. The similar performance of the bare membrane during operation with temperature steps and during temperature ramping indicates no change in permeation when comparing the latter rapid measurements with those obtained during more time demanding stepwise temperature changes. We reported previously [19] that BSCFO material is susceptible to a slow decline in permeation performance when operating the membrane at temperature lower than 1023 K for several days. However, well matching data obtained in both modes of operation allowed to determine unambiguously the apparent activation energy for oxygen permeation at steady state performance of the membrane reported in the following. Comparing the oxygen permeation performance of the different membranes the deposition of Pd nano cluster on BSCFO lead to a slightly increased oxygen flux with generally unchanged temperature dependence. The V/MgO micron grain surface modification caused a pronounced increase in oxygen permeation, i.e. approximately doubled fluxes. Moreover, two different temperature domains become distinguishable as the permeation flux depends strongly on the temperature below 1000 K and becomes less distinctly increased when rising the temperature beyond.

In order to quantify the latter observations the overall apparent activation energies of oxygen permeation were estimated. Fig. 2 shows the logarithm of the oxygen permeation flux as a function of the reciprocal temperature for the bare BSCFO membrane. The apparent activation energy is found to be 83.7 kJ mol^{-1} at lower temperature, which is significantly higher than 46.3 kJ mol^{-1} at higher temperature. The intersection of these two domains takes place at slightly above 1000 K. A comparable behavior has already been observed by other authors studying other membrane compositions [27], although most studies focused on higher temperatures. Moreover, activation energies at high temperatures calculated in this work are considerably lower than those derived from LSCFO types [21], but agree well with previous reports for BSCFO material [22]. No further analysis was performed for the case of the Pd nano cluster modified membrane as this catalyst enhance oxygen permeation only slightly with comparable characteristics in temperature dependency. Table 1 reports the results of similar evaluations for a MgO and V/MgO micron grain modified membrane. The V/MgO catalyst influences strongly the oxygen permeation causing at temperatures below 1000 K a rise in apparent activation energy to 133.6 kJ $mol-^{-1}$, while the activation energy decreases to 29.0 kJ mol^{-1} at higher temperatures. This might be related to a direct action of the catalyst, e.g. causing at lower temperature an oxygen re-adsorption whereas it desorbs oxygen at higher temperature. However, a direct altering of the membrane could have also occurred. Hence, reference studies were performed with samples having in place of V/MgO only MgO deposited. In the latter case, the apparent activation energy at high temperature remained with 45.8 kJ mol^{-1} close to the value observed for bare BSCFO. An almost unchanged value while having a chemical composition close to the catalytic sample allowed to conclude that the observed changes for V/MgO modified samples are effectively related to a direct action of the catalyst.

Table 1
Activation energies of oxygen permeation for a bare, MgO and V/MgO micron grain modified membrane

Membrane type	Apparent activation energy (kJ mol^{-1})	
	Low temperature	High temperature
Bare	83.7 (873–990 K)	46.3
MgO	n.d.[a]	45.8
V/MgO	133.6 (973–998 K)	29.0

[a] n.d.: value was not to determinate.

3.2. Oxygen permeation: modeling

The change in activation energy dividing two temperature regions might be related to a shift of the elementary step limiting the overall oxygen permeation. In order to obtain more information on the oxygen permeation and possibly negating rate limitations by certain steps, it was attempted to model the overall permeation. Several models [23–27] have been tested, assuming control of the oxygen flux by different elementary steps, either volume diffusion of oxygen ions (or vacancies) in the membrane bulk or the exchange of oxygen between gas-phase and surface. Generally, it was observed that the permeation was insufficiently described by the theory of Wagner [26]. Indeed, one of the basic assumptions of this model is an equilibration of the oxygen exchange at both surfaces. Hence, it appears that these exchanges are kinetically limited and thus must be taken into account for modeling the oxygen flow. The best match between calculated fluxes and experimental data was observed for the model developed by Xu and Thomson [27] taking surface exchanges explicitly into account. This model uses the expression in Eq. (1) to correlate oxygen flow $J(O_2)$ across a membrane with thickness L at varying partial pressures of oxygen on both sides ($p'(O_2)$ and $p''(O_2)$). Model parameters are the diffusion coefficient of oxygen vacancies in the bulk (D_V), and the rate constants of the surface exchange, i.e. k_f for the adsorption following Eq. (2) in forward direction and k_r for the desorption following Eq. (2) in backward direction:

$$J(O_2) = \frac{k_r(p'(O_2)^{0.5} - p''(O_2)^{0.5})}{2Lk_f/D_V(p'(O_2)p''(O_2))^{0.5} + (p'(O_2)^{0.5} + p''(O_2)^{0.5})} \quad (1)$$

The exchange of oxygen between gas-phase and surface is assumed to proceed according to the following equation in Kröger-Vink notation:

$$0.5O_2 + V_O^{\bullet\bullet} \underset{k_r}{\overset{k_f}{\rightleftarrows}} O_O^x + 2h^\bullet \quad (2)$$

Furthermore, it is assumed that the temperature dependence of model parameters is of Arrhenius type, i.e. that the following Eqs. (3) and (4) are valid:

$$k_x = k_{x,0}\exp\left(-\frac{E_{a,x}}{RT}\right) \quad (3)$$

and

$$D_V = D_{V,0}\exp\left(-\frac{E_{a,V}}{RT}\right) \quad (4)$$

The parity plot presented in Fig. 3 indicates the satisfactory matching of experimental data and model predictions. Kinetic parameters of the oxygen desorption could be estimated to 1.3×10^{-3} mol cm^{-2} s^{-1} for the pre-exponential coefficient $k_{r,0}$ and to 65 kJ mol^{-1} for the activation energy $E_{a,r}$. The determined activation energy appears quite small compared to a value of 241 kJ mol^{-1} reported for $La_{0.6}Sr_{0.4}Co_{0.2}Fe_{0.8}O_{3-\delta}$ [27]. However, this might be explained by the fact that a higher permeable membrane should also allow an enhanced release of oxygen. This is also in line with the above presented fact that the apparent activation energies for oxygen permeation are substantially lower for BSCFO. Unfortunately, values for D_V and k_f could not be estimated independently as the limited range of temperatures and oxygen partial pressures did not allow to decouple those parameters.

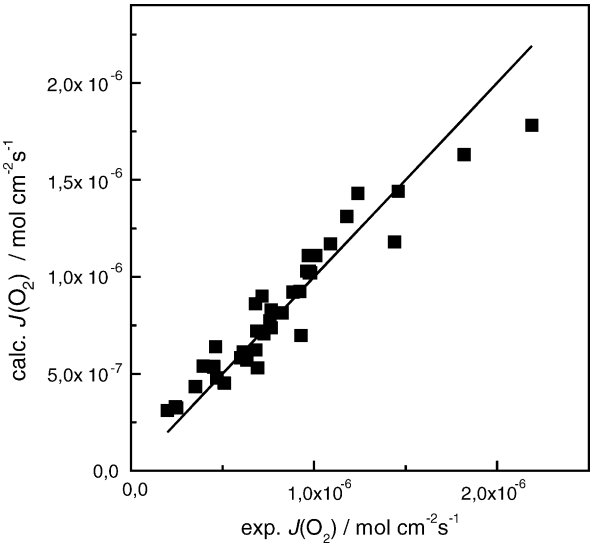

Fig. 3. Parity plot of the experimental and the model predicted oxygen permeation fluxes using the model of Xu and Thomson [27].

In order to elucidate the phenomena of a slow decrease in permeability observed for BSCFO at operating temperatures below 1023 K [19], a temperature programmed XRD study was conducted. It was suspected that the deactivation could relate to structural changes of the material at lowered temperatures, however, possibly only occurring in surface near regions. Fig. 4 presents the diffraction patterns of

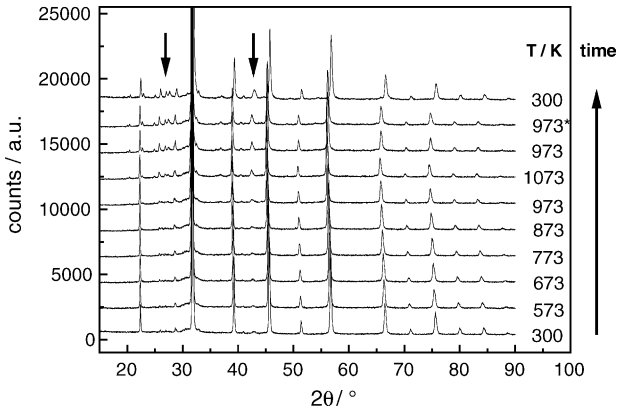

Fig. 4. Diffraction patterns of temperature-programmed XRD characterization of BSCFO powder. Temperature was stepwise increased to 1073 K and then returned to room temperature with a step time of 2 h, except (*) recorded after holding 973 K for 12 h.

BSCFO powder samples in air on increasing stepwise the temperature to 1073 K and back to ambient conditions. The diffraction patterns recorded between 973 and 1073 show the appearance of a second phase, i.e. reflexes at 25–30° and 42.5°, which could not be identified yet. Descending in temperature to 973 K and holding these conditions for another 12 h yielded even more intense reflexes, hence indicating an ongoing formation of the non-perovskite phase. However, the initially pure BSCFO structure was obtained by a synthesis involving calcination at 1173 K in air. It is therefore plausible to conclude that the secondary phase becomes only thermodynamically stable at temperatures below 1050 K. On the other hand, at temperatures above 1050 K, i.e. during synthesis or membrane operation at sufficiently high temperature, a pure perovskite structure becomes favored, explaining the long-term stable oxygen permeation under those conditions.

3.3. Oxygen permeation: long-term stability

Despite of the fact that the secondary phase could not be identified, previous work [19] indicated an altering of the chemical composition of only a thin surface layer at the permeation side of the membrane. Hence it seemed probable that a deposition of surface catalysts could influence the membrane properties and possibly help to overcome the deactivation at lowered temperatures. Fig. 5 reports the oxygen permeation fluxes observed during a study of a V/MgO micron grain modified membrane lasting 23 days. The stability of O_2 permeability was monitored by continuously recording the permeation flux during cyclic changes of the temperature within the range of 950–1075 K. No rapid decline in performance stability was observed when decreasing the membrane temperature down to 950 K. During 1 day of operation permeation fluxes remained almost constant. However, operating the membrane for 14 days at 950 K caused a loss in permeability as a temperature of 1000 K was required to reestablish the flux initially observed at 950 K. On the other hand, at temperatures higher than 1050 K no decline in permeability was observable. Comparing the behavior of the V/MgO catalytic modified membrane with a bare sample [19] it is apparent that the modification leads to a strongly enhanced performance stability at lower operation temperatures. Besides increasing the performance of a membrane [28–30], this action of a surface catalyst might be crucial in future applications.

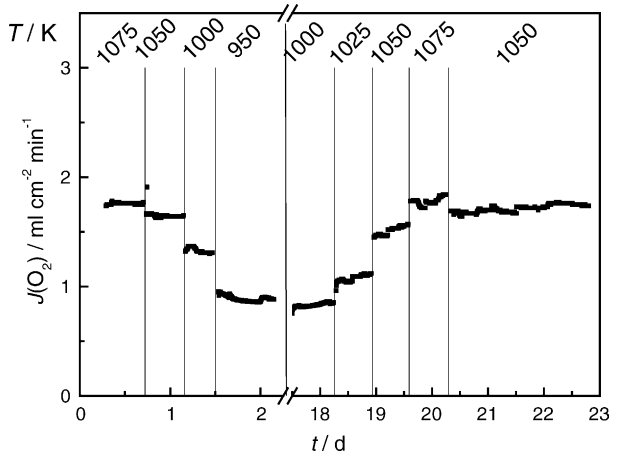

Fig. 5. Oxygen permeation fluxes recorded during a long-term study of a V/MgO micron grain modified BSCFO membrane at different temperatures.

3.4. ODHE performances

Fig. 6a outlines the conversion of ethane as a function of temperature, Fig. 6b presents the observed selectivity towards ethylene. In the case of the bare membrane conversion increased almost linearly with temperature to reach about 70% at 1080 K while selectivity declined slightly. In all cases ethylene selectivity remained however higher than 92%. These observations agree very well with a report were authors used a similar membrane [16] and reflect at lowered temperatures results with a different type of

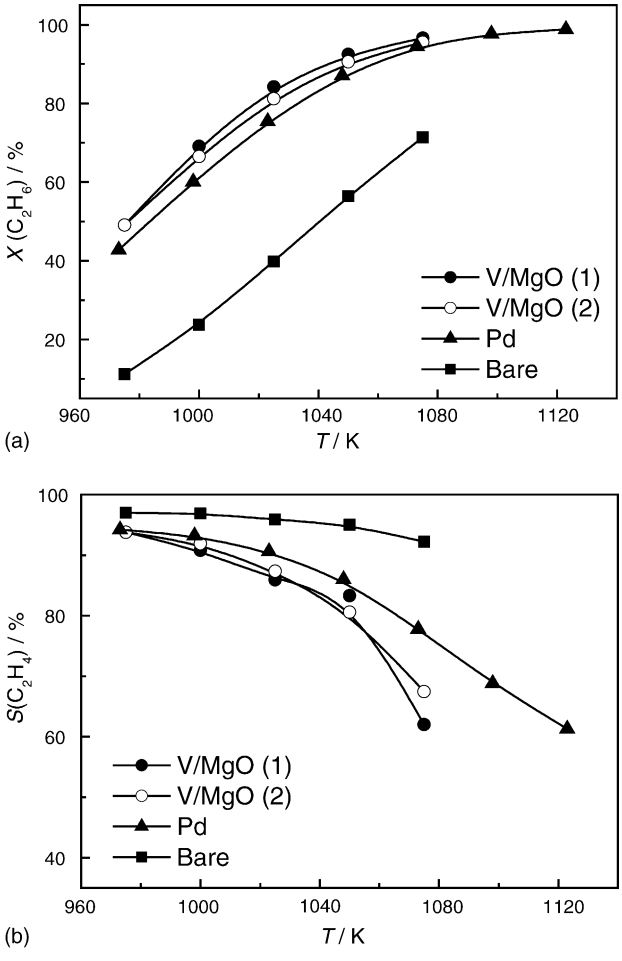

Fig. 6. Ethane conversion (a) and ethylene selectivity as a function of temperature for a bare (■), Pd nano cluster modified (▲) and V/MgO micron grain modified (●,○) membrane. The air side compartment was fed with 50 ml min^{-1} at total pressure of 1.2 bar, the reaction side was supplied with 37 ml min^{-1} C_2H_6 in He at C_2H_6 partial pressure of 0.25 bar.

MIEC membrane [15]. Other products detected in small quantities were CO, CO_2, CH_4 and in larger quantities H_2. No oxygen was observed in phase gas during experiments corresponding to a total consumption of oxygen crossing the membrane. Moreover, there were neither coke deposits observed after one month of use under various conditions nor a deactivation of the CMR. The absence of coking needs to be especially underlined as it is not needed to add steam to the hydrocarbon feed. Reference experiments in a conventional flow-through reactor using either an inert or a BSCFO powder bed without oxygen supply indicated also an ethylene formation, but a fast deactivation (BSCFO) as well as important coke deposition (both cases) were encountered.

In the case of catalyst modified membranes, a strong increase in performance was observed. In the case of V/MgO two experiments carried out with distinct membranes confirmed good reproducibility. Particularly at low temperature conversion rose by a factor 4 compared to the performance of the bare membrane. Contra dictionary to the observations for oxygen permeation, V/MgO and Pd modified samples showed below 1050 K only minor differences. On the other hand, the increase in activity for modified membranes was accompanied by a slight decline in ethylene selectivity. However, values well above 80% were obtained for temperatures up to 1050 K. Beyond that temperature ethylene selectivity decreased, especially in the case of a V/MgO catalyst being applied.

Fig. 7 presents the yield of ethylene over the three types of membranes as a function of temperature. Firstly it is remarkable that both catalytically modified membranes allow to obtain yields of about 75%. Secondly it is noteworthy that in comparison to a bare membrane operational points of equal performance are shifted to about 60 K lower temperatures. This leads to a maximum ethylene yield at 1040 K for the V/MgO modified membrane and at 1050 K for the Pd modified membrane. A clear beneficial action of surface catalysts, previously reported to enhance oxygen permeability [28–30], has therefore been established for the selective hydrocarbon conversion. However, further work is required in order to elucidated the involved reaction mechanism. As a matter of fact a substantial amount of hydrogen is formed as by-product which would indicate that the reaction is not exclusively occurring via the conventional ODHE oxidative pathway, but could also significantly proceed via gas-phase dehydrogenation. Indeed, a reaction mechanism involving the formation of C_2H_5 radicals has already been proposed in ODHE [9] and these highly active species could drive after desorption from the catalyst a dehydrogenation in gas-phase. However, definitive conclusions require further work targeting on mechanistic aspects of the reaction and is subject of an ongoing study.

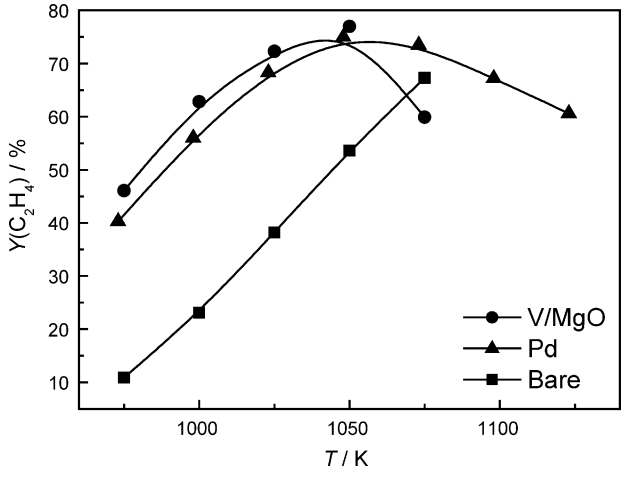

Fig. 7. Ethylene yield as a function of temperature for a bare (■), Pd nano cluster modified (▲) and V/MgO micron grain modified (●) membrane.

4. Conclusion

Results in this work underline that a use of MIEC membranes makes it possible to combine the advantages of ODHE, i.e. long-term stable operation, and steam cracking, i.e. high ethylene yield. Especially a modification of the membrane surface with suitable catalysts makes it possible to improve strongly ethylene yields as compared to a simple bare membrane. Under permeation conditions oxygen fluxes were enlarged by a factor of about two. In view of the fact that other perovskite formulations, e.g. LSCFO [28] or CTFO [29], also have been reported to become limited by surface exchange processes, catalytic surface modifications are of general interest. This holds especially when future developments would decrease membrane thicknesses, i.e. obtain systems with less bulk transfer residence, that would reinforce the need for enhanced transfer rates between surface and gas-phase. On the other hand, calculated oxygen fluxes under conditions of the (O)DHE did not increase to an extend that it is safe to exclude any resistance by the bulk transport. Hence, taking this observation into account the reported highly efficient (O)DHE reaction proceeds in a temperature range with mixed control of the permeation rate. Thus, both the migration of oxygen ions in the bulk by diffusion and the surface exchange or reaction at air and especially permeate side could limit the CMR performance.

Acknowledgement

The authors gratefully acknowledge the financial support granted by the EC programme ‘CERMOX’ (G55RD-CT-2000-0035).

References

[1] H. Zimmermann, R. Walzl, 6th ed., Ethylene in Ullmann’s Encyclopaedia of Industrial Chemistry, 12, Wiley-VCH, Weinheim, 2003, pp. 531–583.

[2] M. McCoy, M. Reisch, A.H. Tullo, P.L. Short, A.M. Thayer, J.-F. Tremblay, W.J. Storck, Facts and figures for the chemical industry: production, Chem. Eng. News 81 (27) (2003) 51–61.
[3] K.M. Sundaram, J.M. Fernandez-Baujin, M.J. Maddock, High selective gas cracking coils for olefins production, Paper no. T-1-89, presented at the UPSIDC, New Delhi, India (18.02.1989) and paper presented at ACHEMA (12.06.1991).
[4] K.M. Sundaram, J.V. Albano, K. Goldmann, Erdöl Erdgas Kohle 111 (1995) 125–129.
[5] J.M. López Nieto, P. Botella, P. Concepción, A. Dejoz, M.I. Vázquez, Catal. Today 91–92 (2004) 241–245.
[6] Y. Liu, P. Cong, R.D. Doolen, S. Guan, V. Markov, L. Woo, S. Zeyß, U. Dingerdissen, Appl. Catal. A 254 (2003) 59–66.
[7] S.A.R. Mulla, O.V. Buyevskaya, M. Baerns, J. Catal. 197 (2001) 43–48.
[8] G. Grubert, E. Kondratenko, S. Kolf, M. Baerns, P. van Geem, R. Parton, Catal. Today 81 (2003) 337–345.
[9] S. Gaab, M. Machli, J. Find, R.K. Grasselli, J.A. Lercher, Top. Catal. 23 (2003) 151–158.
[10] E. Heracleous, J. Vakros, A.A. Lemonidou, Ch. Kordulis, Catal. Today 91–92 (2004) 289–292.
[11] B. Silberova, R. Burch, A. Goguet, C. Hardacre, A. Holmen, J. Catal. 219 (2003) 206–213.
[12] P.N. Dyer, M.F. Carolan, D. Butt, R.H.E. van Doorn, R.A. Cutler, Mixed conducting membranes for syngas production', US Patent 6,492,290, 2002.
[13] A.C. Bose, R.E. Richards, A.F. Sammells, M. Schwartz, Desalination 144 (2002) 91–92.
[14] H.J.M. Bouwmeester, Catal. Today 82 (2003) 141–150.
[15] F.T. Akin, Y.S. Lin, J. Membr. Sci. 209 (2002) 457–467.
[16] H. Wang, Y. Cong, W.S. Yang, Catal. Lett. 84 (2002) 101–106.
[17] Z.P. Shao, G.X. Xiong, H. Dong, W.S. Yang, L. Lin, Separ. Purif. Technol. 25 (2001) 97–116.
[18] Z.P. Shao, W.S. Yang, Y. Cong, H. Dong, J.H. Tong, G.X. Xiong, J. Membr. Sci. 172 (2000) 177–188.
[19] A.C. van Veen, M. Rebeilleau, D. Farrusseng, C. Mirodatos, Chem. Commun. (2003) 32–33.
[20] L. Albaric, N. Hovnanian, A. Julbe, G. Volle, Polyhedron 20 (2001) 2261–2268.
[21] J.E. ten Elshof, H.J.M. Bouwmeester, H. Verweij, Appl. Catal. A 130 (1995) 195–212.
[22] Z.P. Shao, H. Dong, G.X. Xiong, Y. Cong, W.S. Yang, J. Membr. Sci. 183 (2001) 181–192.
[23] S. Kim, Y.L. Yang, R. Christoffersen, A.J. Jacobson, Solid State Ionics 104 (1997) 57–65.
[24] S. Kim, Y.L. Yang, R. Christoffersen, A.J. Jacobson, Solid State Ionics 109 (1998) 187–196.
[25] H.J.M. Bouwmeester, H. Kruidhof, A.J. Burggraaf, P.J. Gellings, Solid State Ionics 53–56 (1992) 460–468.
[26] C. Wagner, Prog. Solid State Chem. 10 (1975) 3–16.
[27] S.J. Xu, W.J. Thomson, Chem. Eng. Sci. 54 (1999) 3839–3850.
[28] S. Lee, K.S. Lee, S.K. Woo, J.W. Kim, T. Ishiara, D.K. Kim, Solid State Ionics 158 (2003) 287–296.
[29] F.M. Figueiredo, V.V. Kharton, A.P. Viskup, J.R. Frade, J. Membr. Sci. 236 (2004) 73–80.
[30] D. Farrusseng, A. van Veen, M. Rebeilleau, C. Mirodatos, S. Rushworth, Patent filed the 28th August 2003 at the French Patent Office no. 03 10 258.